Electronic Supplementary Material (ESI) for Chemical Science.

Supporting Information

Achieving an Exceptionally High Loading of Isolated Cobalt Single Atoms on Porous Carbon Matrix for Efficient Visible-Light-Driven Photocatalytic Hydrogen Production

Rui Shi,[1,#] Chengcheng Tian,[2,#] Xiang Zhu,[2,3,4,*] Cheng-Yun Peng,[1] Bingbao Mei,[5] Lin He,[3,*] Xian-Long Du,[5] Zheng Jiang,[5] Yong Chen[1,*] and Sheng Dai[2,*]

[1] Key Laboratory of Photochemical Conversion and Optoelectronic Materials & HKU-CAS Joint Laboratory on New Materials, Technical Institute of Physics and Chemistry, Chinese Academy of Sciences, Beijing 100190, China

[2] Chemical Sciences Division, Oak Ridge National Laboratory, Oak Ridge, TN 37831, USA

[3] State Key Laboratory for Oxo Synthesis and Selective Oxidation, Suzhou Research Institute of Lanzhou Institute of Chemical Physics, Chinese Academy of Sciences, Lanzhou, 730000, China

[4] Department of Chemistry, Texas A&M University, College Station, Texas 77843, USA

[5] Shanghai Synchrotron Radiation Facility, Shanghai Institute of Applied Physics, Chinese Academy of Sciences, Shanghai 201204, China

1. Experimental section

Chemicals and Materials. All materials were from commercial sources and used as received without any further purification. 1,4,5,8,9,12-hexaazatriphenylene hexacarbonitrile (HAT-6CN) was prepared following our previously-reported method.[1]

Characterization. XRD spectra was measured on a Bruker D8-advance diffractometer using Cu Kα (λ=1.54056 Å). The XRD data for indexing and cell-parameter calculation were collected in a scanning mode and a preset time of 1s/step. Steady-state photoluminescence (PL) spectra of the sample were investigated utilizing a Hitachi F-4500 spectrophotometer equipped with a xenon lamp as the excitation light source. Diffuse reflection spectra (DRS) were obtained on a Varian-Cary 5000 UV-Vis-IR spectrophotometer. Transient IR absorption spectra (TIRA) were measured by the pump and probe method. A quantum cascade laser continuously tunable from 4.69 to 4.88 μm (TLC-21045, Daylight Solution) was used as the mid-IR probe light. 355 nm laser pulses from a Nd:YAG laser (Quanta Ray, Spectra Physics) with a pulse duration of 10 ns and a repetition rate of 10 Hz were used to pump an optical parametric oscillator (GWU premiScan-ULD/240, Spectra Physics) that acted as a wavelength-scanning excitation source (the output signal beam was tunable from 410 to 709 nm). X-ray photoelectron spectroscopy (XPS) spectra were recorded on an ESCALABMK Ⅱ X-ray photoelectron spectrometer using Mg as the exciting source. The morphology and lattice fringes were performed by a transmission electron microscope (TEM, JEM 2100 F) with an accelerating voltage of 200 kV. Scanning electron microscope (SEM), energy dispersive X-ray spectroscopy and elemental mapping were taken on Hitachi S-4800 field-emission scanning electron microscope. HRMS (high resolution mass spectra) were obtained on Thermo Scientific Q Exactive mass spectrometer, operated in heated electrospray ionization (HESI) mode, and coupled with Thermo Scientific Ultimate 3000 system. Raman measurements were obtained using a Renishaw InVia-Reflex spectrometer equipped with a notch filter and a CCD detector. Elemental analysis data for samples were obtained using inductively coupled plasma atomic emission spectrometry (ICP-AES Varian 710-OES, USA). N_2 adsorption and desorption curves at 77 K were recorded by ASAP 2020.

The high-angle annular-dark-field scanning transmission electron microscopy (HAADF-STEM) images were performed using a Titan 80-300 STEM operated at 300 KV, equipped with a probe spherical aberration corrector.

X-ray absorption spectra (XAS) measurements were performed on Beam line BL14W1 at the Shanghai Synchrotron Radiation Facility (SSRF) with the electron storage ring operated at 3.5 Gev, equipped with a double Si (111) crystal monochromator. High-order harmonics were inhibited using a harmonic suppression mirror. Two gas-filled ionization chambers were employed to measure the intensities of the incident beam (I_0) and the transmitted beam (I_1) after the sample. XAS data were collected at the Co K-edge in transmission mode. XAS data of reference Co foil was studied under a similar condition. Data reduction and analysis were processed by Athena software.

2. Figures

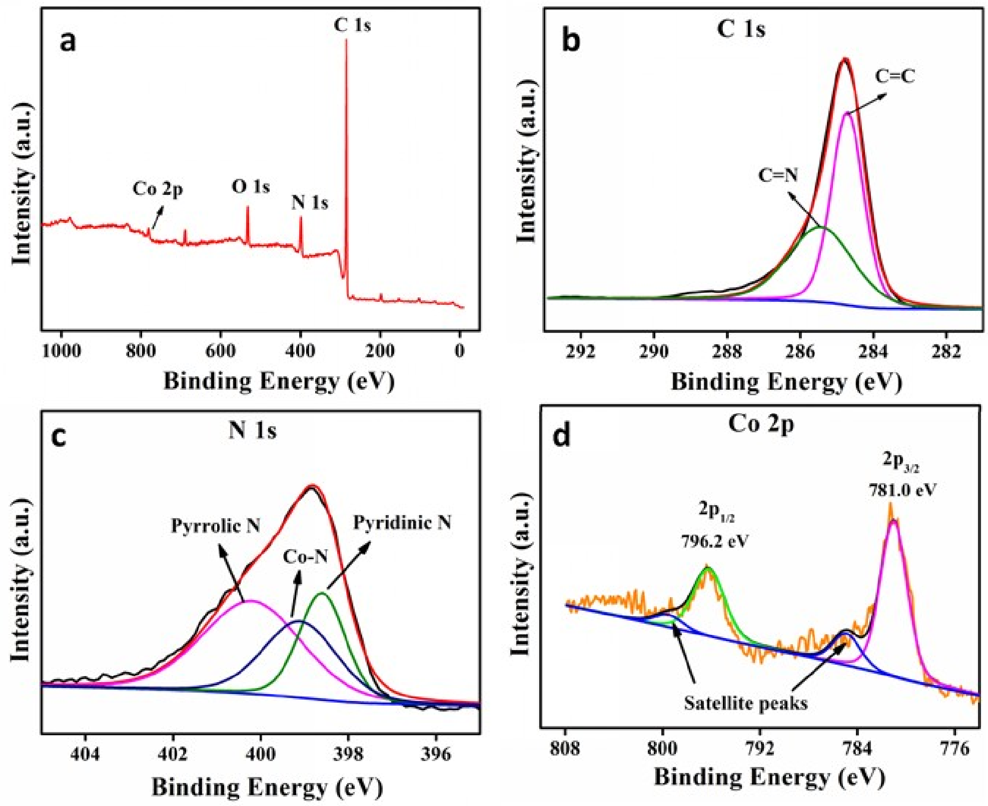

Figure S1. XPS studies of **Co-N-C** [C1s (b), N1s (c), and Co 2P (d)].

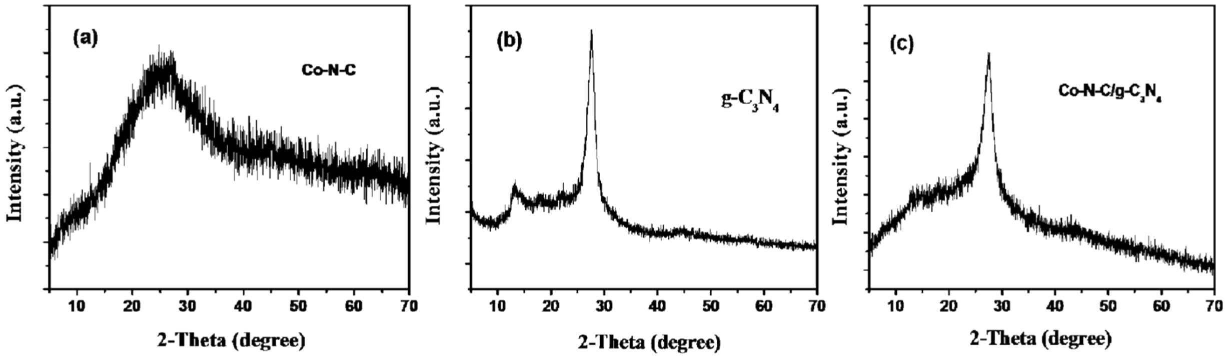

Figure S2. The XRD patterns of **Co-N-C** (a), g-C_3N_4 (b) and **Co-N-C/g-C_3N_4** (c).

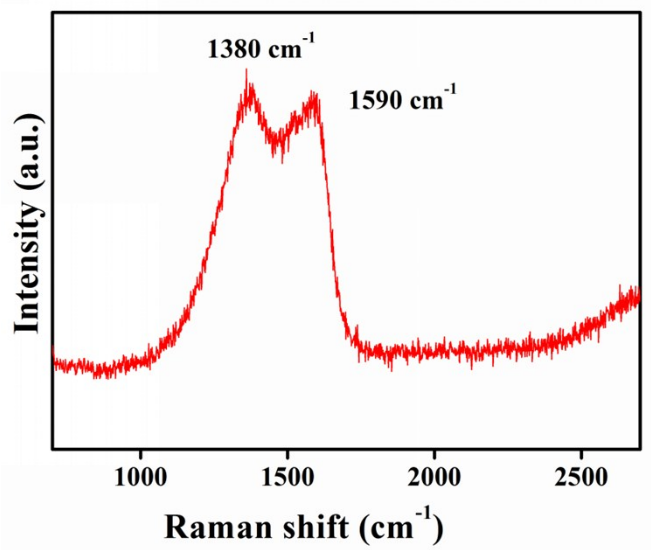

Figure S3. The Raman spectra of **Co-N-C.**

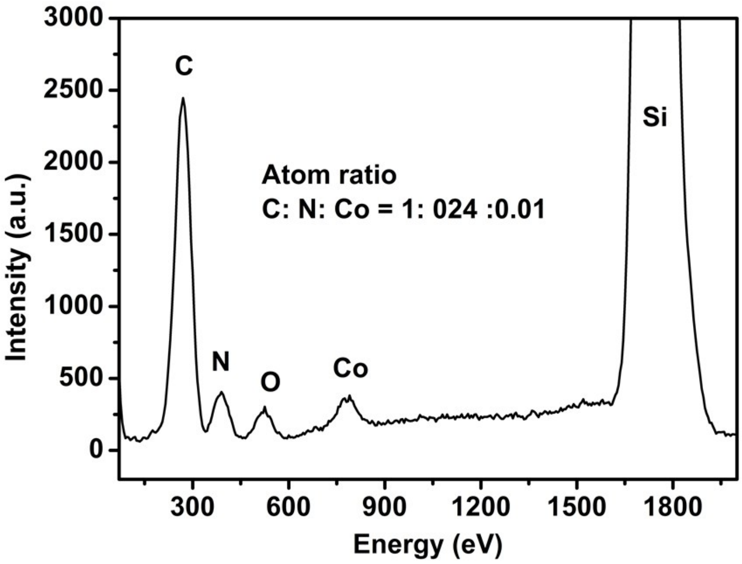

Figure S4. EDX spectrum of **Co-N-C**.

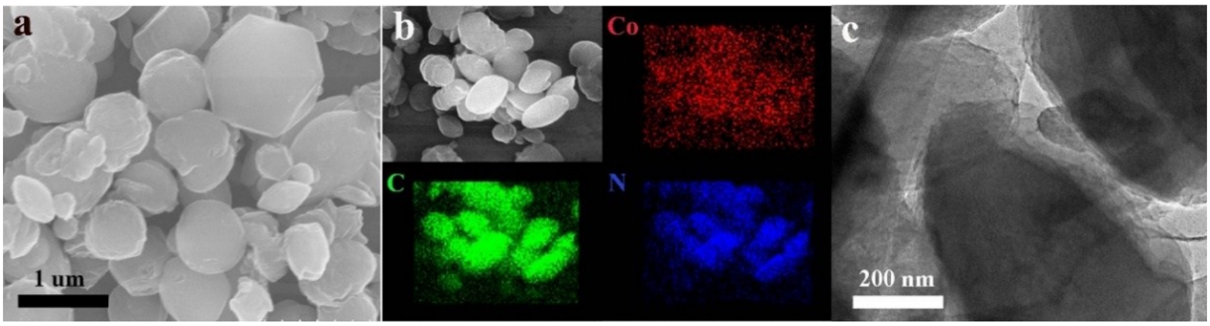

Figure S5. SEM (a), mapping (b) and TEM (c) of **Co-N-C**.

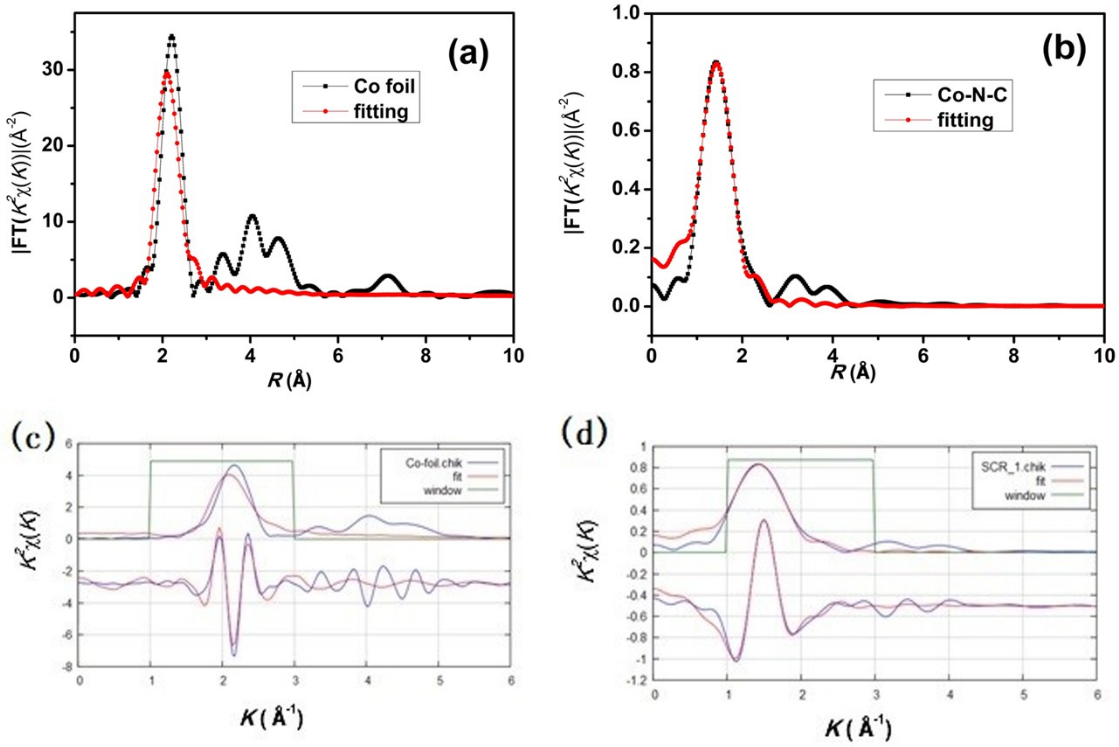

Figure S6. Fourier transform of experimental EXAFS spectra and best fit results for Co foil (a) and **Co-N-C** (b). Fourier transform of EXAFS spectra in R space and the best fitting result for Co foil (c) and **Co-N-C** (d).

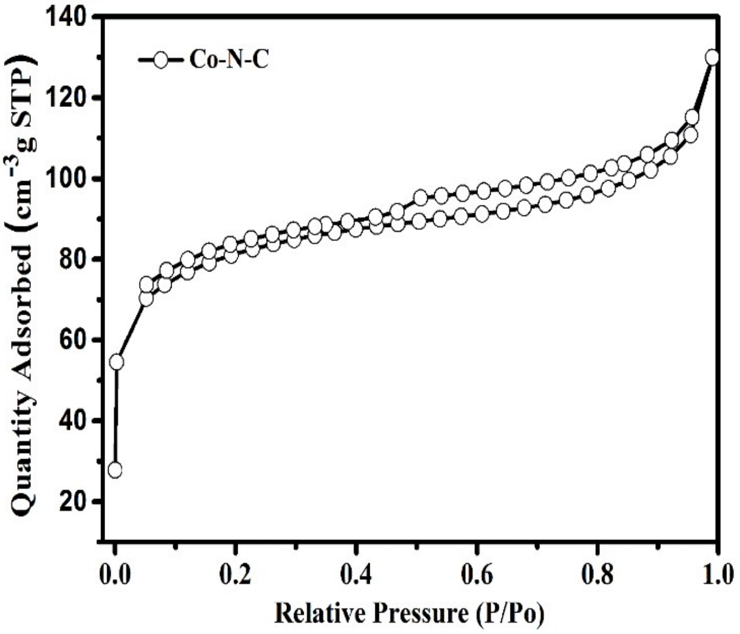

Figure S7. N_2 adsorption-desorption curves for **Co-N-C**, recorded at 77 K.

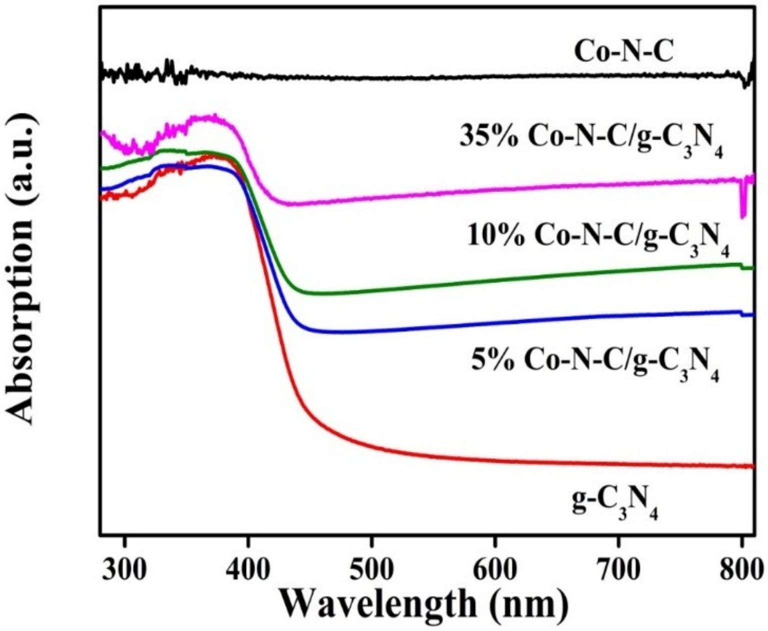

Figure S8. UV-vis diffuse reflectance images of pure g-C_3N_4, **Co-N-C** and **Co-N-C/g-C_3N_4** composites.

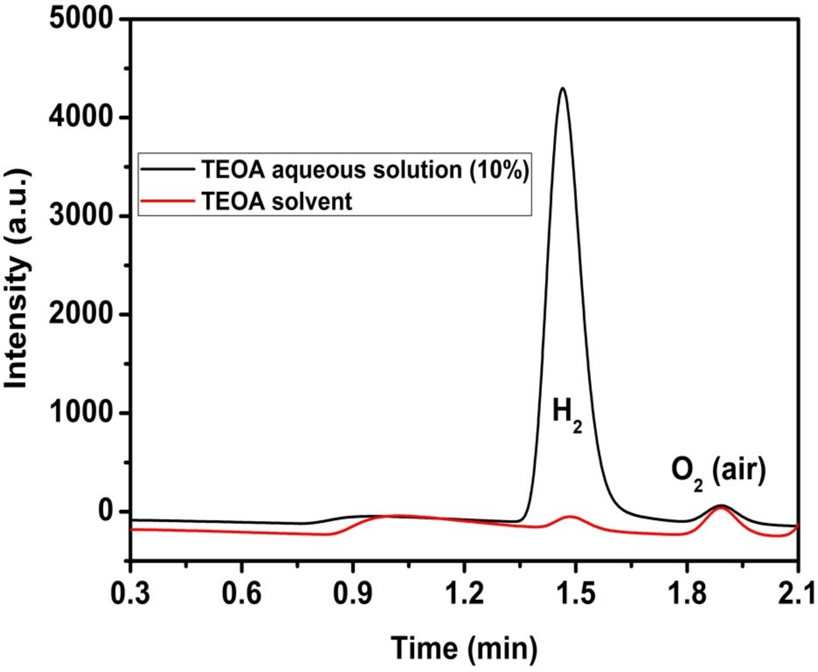

Figure S9. GC signals of photocatalytic H_2 evolution in TEOA aqueous solution (10% in volume) and TEOA solvent.

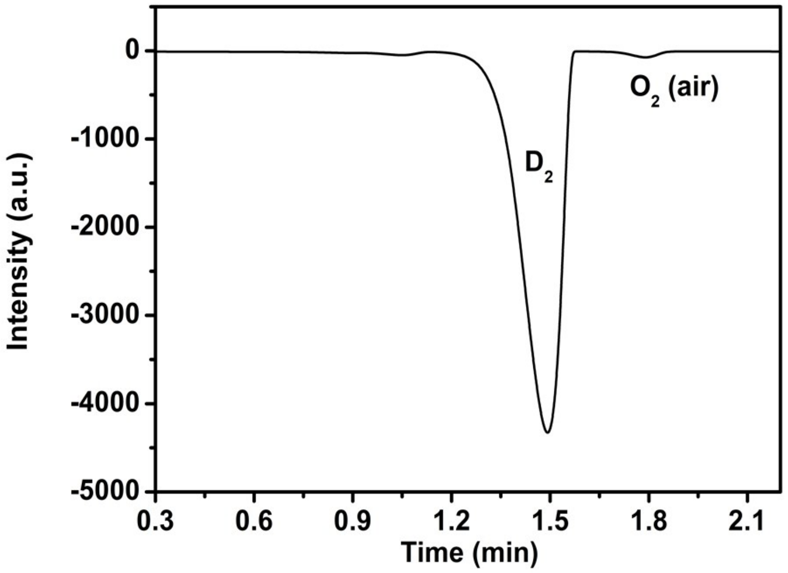

Figure S10. GC signals obtained using He as the carrier gas.

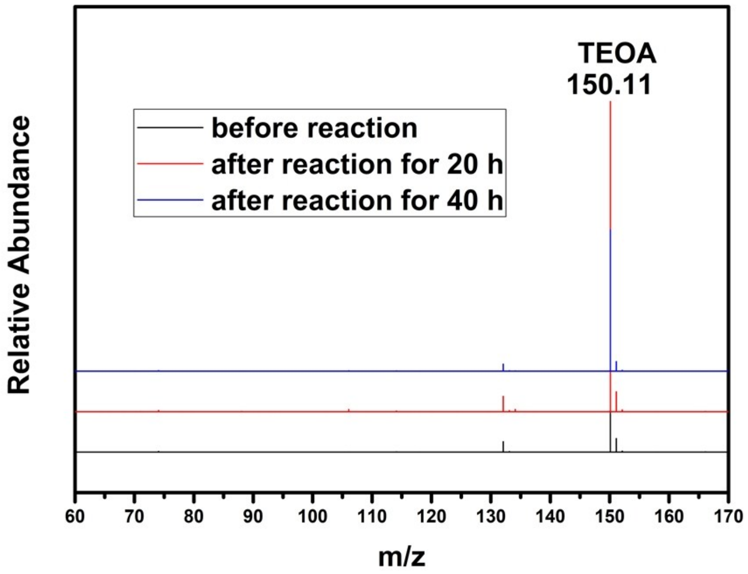

Figure S11. ESA-MS spectra for TEOA after photocatalysis H_2 evolution.

The amount of TEOA in photocatalytic reaction system is 3700 μmol. In order to speed up the ratio of photocatalysis H_2 evolution, the amount of CoN-C/g-C_3N_4 is increased to 10 mg. When photocatalytic reaction time was carried out to 20 h and 40 h, the amount of H_2 produced was 129.2 and 239.5 μmol, respectively. Meanwhile, ESI-MS spectroscopy was applied to monitor the possible degradation product. The results showed that no additional peaks of corresponding oxidation products of TEOA were observed, such as aldehyde and carboxylic acid, which suggest that TEOA is degraded into fragmented molecules after accepting the photogenerated holes.

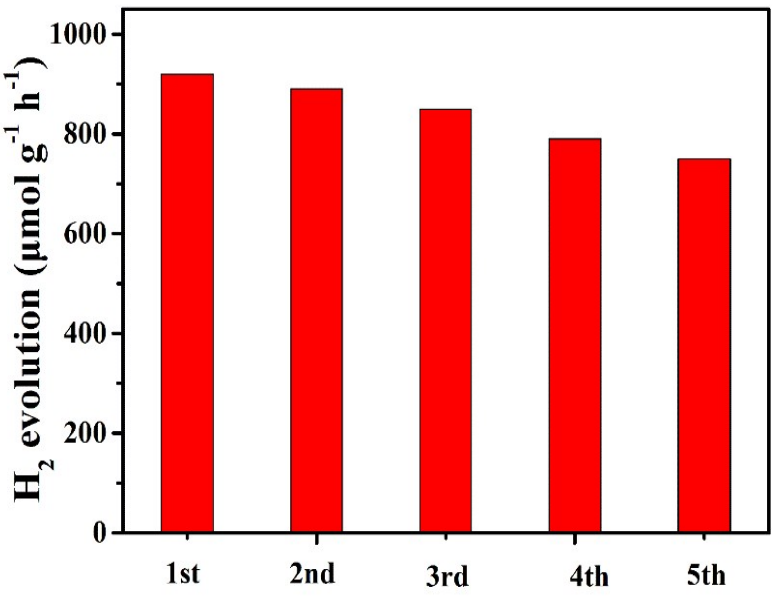

Figure S12. Durability tests for **Co-N-C/g-C$_3$N$_4$** (4 hours per cycle experiment).

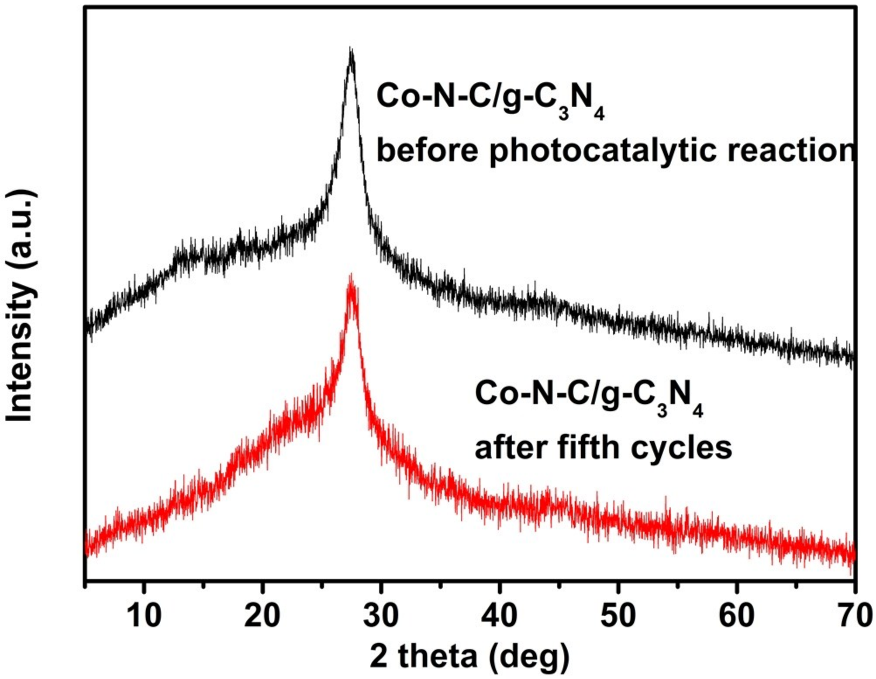

Figure S13. XRD pattern of **Co-N-C/g-C$_3$N$_4$** of before and after photocatalytic reaction.

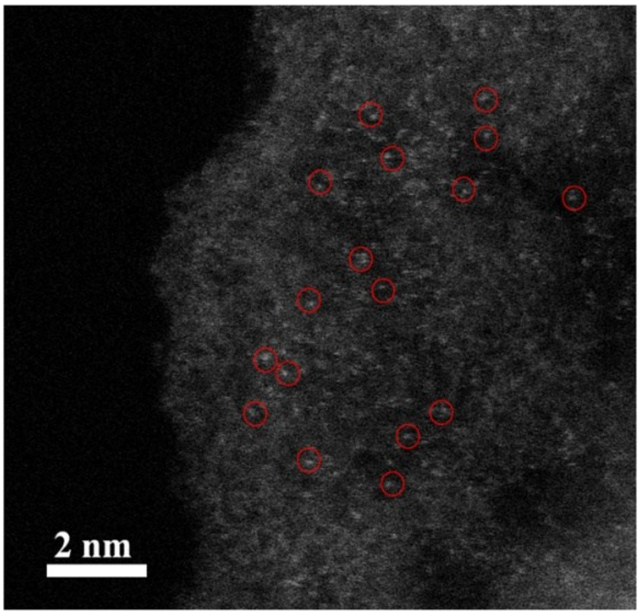

Figure S14. HAADF-STEM image of **Co-N-C/g-C_3N_4** after the photocatalytic reaction.

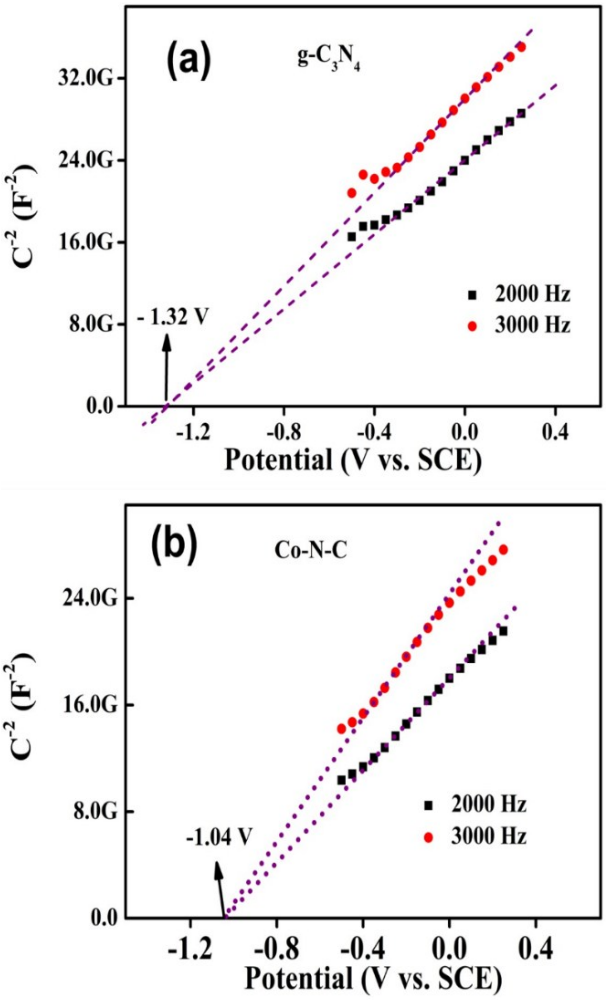

Figure S15. Mott-Schottky plots of g-C_3N_4 (a) and **Co-N-C** (b) in the dark at frequencies of 2000 and 3000 Hz.

3. Scheme S1. Proposed synthesis scheme for the construction of HAT-CTFs from HAT-3CN.

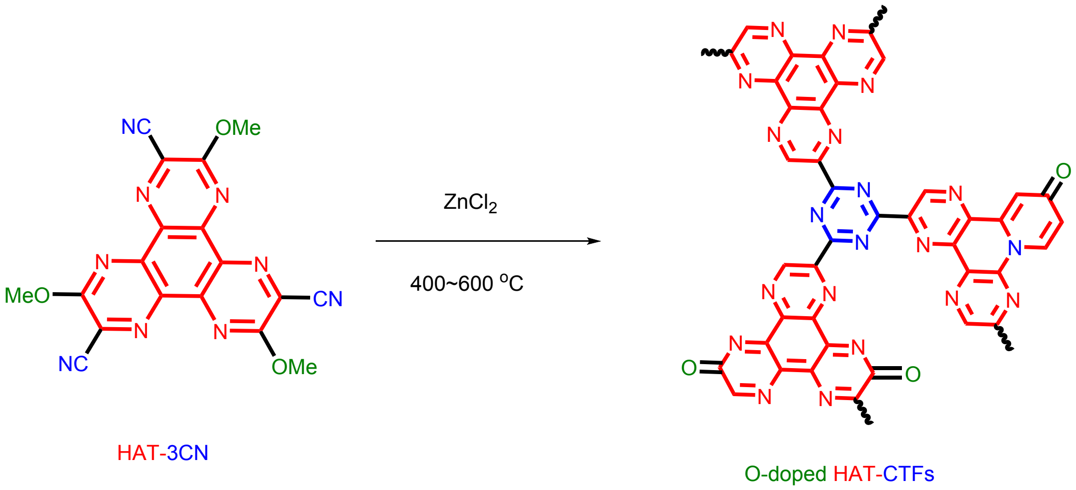

4. Table

Table S1. Co K-edge EXAFS curve fitting parameters.

Sample	Absorption-backscattering pair	*N*	Bond distance	σ^2	ΔE_0 (eV)
Co foil[a]	Co-Co	12	2.21 Å	0.0086	8.21
Co-N-C[b]	Co-N	4	1.46 Å	0.013	2.27

Background removal and normalization procedures were carried out using the Athena software package using standard methods.[1] Data analysis has been performed with the FEFF8 software package. The experimental (k) functions have been extracted from the absorption spectra through a standard procedure of subtraction of the pre-edge and fit evaluated monoatomic background, and normalization to the edge jump. The coordination number for the isolated centers is quantified by least-squares EXAFS curve-fitting analysis.

[a]Fitting range: $1.4 \le R$ (Å) ≤ 2.7

[b]Fitting range: $1.0 \le R$ (Å) ≤ 2.7

N: coordination number

σ^2: XAFS Debye-Waller factor to account for both thermal and structural disorders.

ΔE_0: inner potential correction

Table S2. Lifetimes of TIRA decays of g-C_3N_4, **Co-N-C** and **Co-N-C/g-C_3N_4** under 420 nm and 600 nm irradiation, respectively. [The average lifetime was calculated using equation: $\tau_{av} = (\alpha_1\tau_1^2 + \alpha_2\tau_2^2)/(\alpha_1\tau_1 + \alpha_2\tau_2)$]

Sample	420 nm Irradiation			600 nm Irradiation		
	τ_1 /ps	τ_2 /ps	τ_{av} /ps	τ_1 /ps	τ_2 /ps	τ_{av} /ps
g-C_3N_4	66.1(29%)	747.6(71%)	723.9			
Co-N-C	0.3(88%)	4.6 (12%)	3.2	0.4(83%)	5.2(17%)	3.9
Co-N-C/g-C_3N_4	0.4(83%)	4.7 (17%)	3.4	0.5(78%)	5.6(22%)	4.4

Table S3. Photocatalytic H_2 generation of g-C_3N_4-based heterostructures.

Photocatalysts	**Mass of photocatalyst**	**Reactant solution**	**Light source**	**H_2 generation rate (umol/hg)**	**Refs**
g-C_3N_4	0.002 g	5 mL of triethanolamine aqueous solution (10% in volume)	12 W LED lamp (λ=420 ±10 nm)	22	This paper
Co-N-C/g-C_3N_4	0.002 g	5 mL of triethanolamine aqueous solution (10% in volume)	12 W LED lamp (λ=420 ±10 nm)	1180	This paper
g-C_3N_4	0.05 g	100 mL of triethanolamine aqueous solution (10% in volume)	300 W Xe lamp (λ>420 nm)	200	[2]
g-C_3N_4	0.1 g	100 mL of triethanolamine aqueous solution (10% in volume)	mercury short-arc lamp (500W)	180	[3]
g-C_3N_4	0.1g	100 mL of triethanolamine aqueous solution (10% in volume)	300 W Xe lamp (λ>420 nm)	180	[4]
g-C_3N_4	0.1g	100 mL of triethanolamine aqueous solution (10% in volume)	300 W Xe lamp (420—780 nm)	260	[5]
g-C_3N_4	0.05g	100 mL of triethanolamine	300 W Xe lamp	130	[6]

		aqueous solution (10% in volume)	(λ>420 nm)		
g-C_3N_4	0.3g	400 mL of lactic acid aqueous solution (12.5% in volume)	450W high pressure Hg lamp (436 nm)	37	[7]
g-C_3N_4	0.05g	100 mL of lactic acid aqueous solution (20% in volume)	300 W Xe lamp (λ>420 nm)	49	[8]
Pt/FeO_x/g-C_3N_4	0.1g	100 mL of triethanolamine aqueous solution (10% in volume)	300 W Xe lamp (420—780 nm)	1080	[5]
Pt/g-C_3N_4	0.05g	100 mL of triethanolamine aqueous solution (10% in volume)	300 W Xe lamp (λ>420 nm)	6360	[6]
TiO_2/g-C_3N_4	0.3g	400 mL of lactic acid aqueous solution (12.5% in volume)	450W high pressure Hg lamp (436 nm)	74	[7]
Pt/CeO_2/g-C_3N_4	0.05g	100 mL of lactic acid aqueous solution (20% in volume)	300 W Xe lamp (λ>420 nm)	73	[8]
Pt/MoS_2/g-C_3N_4	0.1g	120 mL of methanol aqueous solution (25% in volume)	300 W Xe lamp (λ>400 nm)	231	[9]
MoS_2/g-C_3N_4	0.01g	10 mL of triethanolamine aqueous solution (10% in volume)	300 W Xe lamp (λ>400 nm)	252	[10]
$Cd_{0.2}Zn_{0.8}S$/g-C_3N_4	0.05	100 mL of 0.1 M Na_2S and Na_2SO_3 aqueous solution	300 W Xe lamp (λ>420 nm)	4160	[11]
$Cd_{0.5}Zn_{0.5}$SQDs/g-C_3N_4	0.02g	100 mL of 0.1 M Na_2S and Na_2SO_3 aqueous solution	300 W Xe lamp (420—786 nm)	33400	[12]
Ag_2S/g-C_3N_4	0.05g	80 mL of methanol aqueous solution (25% in volume)	Four UV-LEDs (3W, 420nm)	200	[13]
WS_2//g-C_3N_4	0.05g	80 mL of methanol aqueous solution (20% in volume)	300 W Xe lamp (λ>420 nm)	101	[14]
Pt/$CaIn_2S_4$/g-C_3N_4	0.05g	80 mL of 0.5 M Na_2S and Na_2SO_3 aqueous	Four UV-LEDs (3W, 420nm)	102	[15]
NiS/CdS/g-C_3N_4	0.05g	100 mL of triethanolamine aqueous solution (10% in volume)	300 W Xe lamp (λ>420 nm)	2560	[16]
$Ni_{12}P_5$/g-C_3N_4	0.05g	80 mL of triethanolamine aqueous solution (15% in	350 W Xe lamp (λ>420 nm)	126	[17]

		volume)			
Pt/CNT/g-C_3N_4	0.1g	100 mL of triethanolamine aqueous solution (10% in volume)	300 W Xe lamp (λ>420 nm)	394	[18]
Pt/Carbon black/g-C_3N_4	0.1g	100 mL of methanol aqueous solution (12% in volume)	(λ>420 nm)	689	[19]
ZIF-8derived carbon/g-C_3N_4	0.1g	300 mL of triethanolamine aqueous solution (10% in volume)	300 W Xe lamp (λ>420 nm)	326	[20]
$Ni(OH)_2$/g-C_3N_4	0.05g	80 mL of triethanolamine aqueous solution (10% in volume)	350 W Xe lamp (λ>400 nm)	152	[21]
PtCo/g-C_3N_4	0.05g	100 mL of triethanolamine aqueous solution (10% in volume)	300 W Xe lamp (λ>400 nm)	960	[22]
PdAu/g-C_3N_4	0.05g	100 mL of triethanolamine aqueous solution (10% in volume)	300 W Xe lamp (λ>400 nm)	326	[23]
Ni/g-C_3N_4	0.05g	100 mL of triethanolamine aqueous solution (10% in volume)	500 W Xe lamp	313	[24]
Ni/g-C_3N_4	0.05g	100 mL of triethanolamine aqueous solution (10% in volume)	500 W Xe lamp	168	[25]
Pt/g-PAN/g-C_3N_4	0.1g	300 mL of triethanolamine aqueous solution (10% in volume)	300 W Xe lamp (λ>400 nm)	370	[26]
NiFe-LDH/g-C_3N_4	0.03g	30 mL of methanol aqueous solution (10% in volume)	125W medium pressure Hg lamp (λ>420 nm)	736	[27]
NiS/CNT/g-C_3N_4	0.05g	100 mL of methanol aqueous solution (10% in volume)	300 W Xe lamp	520	[28]
P25/Au/ g-C_3N_4	0.05g	50 mL of methanol aqueous solution (30% in volume)	300 W Xe lamp	219	[29]
$(FeTPP)_2O$/g-C_3N_4	0.08g	100 mL of methanol aqueous solution (10% in volume)	300 W Xe lamp (λ>420 nm)	500	[30]

Table S4. Photocatalytic H_2 generation of SACs.

Photocatalysts	Mass of photocatalyst	Reactant solution	Light source	H_2 generation rate (umol/hg)	Refs
Co-N-C/g-C_3N_4	0.002 g	5 mL of triethanolamine aqueous solution (10% in volume)	12 W LED lamp (λ=420 ±10 nm)	1180	This paper
Pt/TiO_2	10mg	80 mL of methanol aqueous solution (20% in volume)	300 W Xe lamp	8450	[31]
Co/N-doped graphene/CdS	100mg	100mL of 1.0M $(NH_4)_2SO_3$ aqueous	300 W Xe lamp (λ>420 nm)	13820	[32]
Co/N-doped graphene/TiO_2	25mg	120 mL of ethanol aqueous solution (42% in volume)	300 W Xe lamp	677	[33]
Pt/$(AlOH)_2H_2$TCPP	5mg	20 mL of triethanolamine acetonitrile solution (5% in volume)	300 W Xe lamp (λ>380 nm)	129	[34]
Pt/g-C_3N_4	50mg	200mL of triethanolamine aqueous solution (10% in volume)	300 W Xe lamp	6360	[35]
Pt/Ir-HNTM	50mg	50mL of triethanolamine acetonitrile solution (8% in volume)	300 W Xe lamp (λ>400 nm)	201.9	[36]
Co/P-doped g-C_3N_4	20mg	100 mL water	300 W Xe lamp (λ>420 nm)	126.8	[37]

5. References

1. X. Zhu, C. Tian, G. M. Veith, C. W. Abney, J. Dehaudt, S. Dai, *J. Am. Chem. Soc.* 2016, **138**, 11497-11500.
2. S. B. Yang, Y. J. Gong, J. S. Zhang, L. Zhan, L. L. Ma, Z. Y. Fang, R. Vajtai, X. C. Wang, P. M. Ajayan, *Adv. Mater.* 2013, **25**, 2452-2456.
3. X. C. Wang, K. Maeda, X. F. Chen, K. Takanabe, K. Domen, Y. D. Hou, X. Z. Fu, M. Antonietti, *J. Am. Chem. Soc.* 2009, **131**, 1680-1681.
4. J. S. Zhang, G. G. Zhang, X. F. Chen, L. Mohlmann, G. Dolega, G. Lipner, M. Antonietti,

S. Blechert, X. C. Wang, *Angew. Chem. Int. Ed.* 2012, **51**, 3183-3187.

5. R. Cheng, L. Zhang, X. Fan, M. Wang, M. Li, J. Shi, *Carbon* 2016, **101**, 62-70.
6. X. Li, W. Bi, L. Zhang, S. Tao, W. Chu, Q. Zhang, Y. Luo, C. Wu, Y. Xie, *Adv. Mater.* 2016, **28**, 2427-2431.
7. H. Yan, H. Yang, *J. Alloys Compd.* 2011, **509**, L26-L26.
8. N. Tian, H. Huang, C. Liu, F. Dong, T. Zhang, X. Du, S. Yu, Y. Zhang, *J. Mater. Chem. A* 2015, **3**, 17120-17129.
9. L. Ge, C. Han, X. Xiao, L. Guo, *Int. J. Hydrog. Energy* 2013, **38**, 6960-6969.
10. H. Zhao, Y. Dong, P. Jiang, H. Miao, G. Wang, J. Zhang, *J. Mater. Chem. A* 2015, **3**, 7375-7381.
11. H. Liu, Z. Jin, Z. Xu, *Dalton Trans.* 2015, **44**, 14368-14375.
12. L. Yao, D. Wei, Y. Ni, D. Yan, C. Hu, *Nano Energy* 2016, **26**, 248-256.
13. D. Jiang, L. Chen, J. Xie, M. Chen, *Dalton Trans.* 2014, **43**, 4878-4885.
14. M. S. Akple, J. Low, S. Wageh, A. A. Al-Ghamdi, J. Yu, J. Zhang, Appl. Surf. Sci. 2015, 358, 196-203.
15. D. Jiang, J. Li, C. Xing, Z. Zhang, S. Meng, M. Chen, *ACS Appl. Mater. Interfaces* 2015, 7, 19234-19242.
16. J. Yuan, J. Wen, Y. Zhong, X. Li, Y. Fang, S. Zhang, W. Liu, *J. Mater.Chem. A* 2015, **3**, 18244-18255.
17. J. Wen, J. Xie, R. Shen, X. Li, X. Luo, H. Zhang, A. Zhang, G. Bi, *Dalton Trans.* 2017, **46**, 1794-1802.
18. Y. Chen, J. Li, Z. Hong, B. Shen, B. Lin, B. Gao, *Phys. Chem. Chem. Phys.* 2014, **16**, 8106-8113.
19. Z. Wu, H. Gao, S. Yan, Z. Zou, *Dalton Trans.* 2014, **43**, 12013-12017.
20. F. He, G. Chen, Y. Zhou, Y. Yu, L. Li, S. Hao, B. Liu, *J. Mater. Chem.A* 2016, **4**, 3822-3827.
21. J. Yu, S. Wang, B. Cheng, Z. Lin, F. Huang, *Catal. Sci. Technol.* 2013, **3**, 1782-1789.
22. C. Han, Y. Lu, J. Zhang, L. Ge, Y. Li, C. Chen, Y. Xin, L. Wu, S. Fang, *J. Mater. Chem. A* 2015, **3**, 23274-23282.
23. C. Han, L. Wu, L. Ge, Y. Li, Z. Zhao, *Carbon* 2015, **92**, 31-40.
24. L. Bi, D. Meng, Q. Bu, Y. Lin, D. Wang, T. Xie, *Phys. Chem. Chem. Phys.* 2016, **18**, 31534-31541.
25. L. Bi, D. Xu, L. Zhang, Y. Lin, D. Wang, T. Xie, *Phys. Chem. Chem. Phys.* 2015, **17**, 29899-29005.

26. F. He, G. Chen, Y. Yu, S. Hao, Y. Zhou, Y. Zheng, *ACS Appl. Mater. Interfaces* 2014, **6**, 7171-7179.
27. S. Nayak, L. Mohapatra, K. Parida, *J. Mater. Chem. A* 2015, **3**, 18622-18635.
28. Y. Zhong, J. Yuan, J. Wen, X. Li, Y. Xu, W. Liu, S. Zhang, Y. Fang, *Dalton Trans.* 2015, **44**, 18260-18269.
29. W. Zhao, L. Xie, M. Zhang, Z. Ai, H. Xi, Y. Li, Q. Shi, J. Chen, *Int. J. Hydrog. Energy* 2016, **41**, 6277-6287.
30. D. H. Wang, J. N. Pan, H. H. Li, J. J. Liu, Y. B. Wang, L. T. Kang, J. N. Yao, *J. Mater. Chem. A* 2016, **4**, 290-296.
31. Y. Sui, S. Liu, T. Li, Q. Liu, T. Jiang, Y. Guo, J. Luo, *J. Catal.* 2017, **353**, 250-255.
32. Q. Zhao, W. Yao, C. Huang, Q. Wu, Q. Xu, *ACS. Appl. Mater. Interfaces* 2017, **9**, 42734-42741.
33. L. Yi, F. Lan, J. Li, C. Zhao, *ACS Sus. Chem. Eng.* 2018, **6**, 12766-12775.
34. X. Fang, Q. Shang, Y. Wang, L. Jiao, T. Yao, Y. Li, Q. Zhang, Y. Luo, H. Jiang, *Adv. Mater.* 2018, **30**, 1705112.
35. X. Li, W. Bi, L. Zhang, S. Tao, W. Chu, Q. Zhang, Y. Luo, C. Wu, Y. Xie, *Adv. Mater.* 2016, **28**, 2427-2431.
36. T. He, S. Chen, B. Ni, Y. Gong, Z. Wu, L. Song, L. Gu, W. HU, X. Wang, *Angew. Chem*. 2018, **130**, 3551-3556.
37. W. Liu, L. Cao, W. Cheng, Y. Cao, X. Liu, W. Zhang, X. Mou, L. Jin, X. Zheng, W. Che, Q. Liu, T. Yao, S. Wei, *Angew. Chem*. 2017, **129**, 9440-9445.